

Published in final edited form as:

Nat Biotechnol. 2013 December ; 31(12): 1119–1125. doi:10.1038/nbt.2727.

Chromosome-scale scaffolding of *de novo* genome assemblies based on chromatin interactions

Joshua N. Burton¹, Andrew Adey¹, Rupali P. Patwardhan¹, Ruolan Qiu¹, Jacob O. Kitzman¹, and Jay Shendure¹

¹Department of Genome Sciences, University of Washington, Seattle, WA 98115, USA

Abstract

Genomes assembled *de novo* from short reads are highly fragmented relative to the finished chromosomes of *H. sapiens* and key model organisms generated by the Human Genome Project. To address this, we need scalable, cost-effective methods enabling chromosome-scale contiguity. Here we show that genome-wide chromatin interaction datasets, such as those generated by Hi-C, are a rich source of long-range information for assigning, ordering and orienting genomic sequences to chromosomes, including across centromeres. To exploit this, we developed an algorithm that uses Hi-C data for ultra-long-range scaffolding of *de novo* genome assemblies. We demonstrate the approach by combining shotgun fragment and short jump mate-pair sequences with Hi-C data to generate chromosome-scale *de novo* assemblies of the human, mouse and *Drosophila* genomes, achieving – for human – 98% accuracy in assigning scaffolds to chromosome groups and 99% accuracy in ordering and orienting scaffolds within chromosome groups. Hi-C data can also be used to validate chromosomal translocations in cancer genomes.

The Human Genome Project (HGP) defined and achieved high standards for the *de novo* assembly of reference genomes for *H. sapiens* and key model organisms. For example, the public draft human genome, reported in 2001, contained 90% of the euchromatic sequence with an N50 (defined as the length L at which 50% of sequence is in contigs of length L) of 82 kilobases (Kb)^{1,2}. The finished human genome, reported in 2004, contained 99% of the euchromatic sequence with an N50 of 38.5 megabases (Mb) and an error rate of 1 event per 100,000 bases². At both stages, nearly all sequences were assigned, ordered and oriented to chromosomes, although many errors were corrected during finishing².

Correspondence to: Jay Shendure (shendure@uw.edu) Joshua Burton (jnburton@uw.edu).

Author Contributions

J.N.B., A.A., J.O.K. and J.S. conceived and designed the study. J.N.B. designed and wrote the *LACHESIS* software. J.N.B. and R.P.P. performed the *de novo* assemblies. R.Q. conducted the HeLa Hi-C experiments. A.A. analyzed the HeLa Hi-C data. J.N.B., A.A. and J.S. prepared the manuscript. J.S. supervised the study.

Competing Financial Interests

The authors are in the process of filing a provisional patent application on this method. J.S. is a member of the scientific advisory board or serves as a consultant for Adaptive Biotechnologies, Ariosa Diagnostics, Stratos Genomics, GenePeeks, Gen9, Good Start Genetics and Rubicon Genomics.

Accession Codes

The HeLa associated genomic datasets described in this manuscript are available via the database of Genotypes and Phenotypes (dbGaP) as a substudy of the HeLa Cell Genome Sequencing Studies, phs000640.

Massively parallel DNA sequencing technologies produce billions of short reads per instrument run at a very low cost per sequenced base, empowering a wide range of experiments^{3,4}. However, although extensive progress has been made in developing algorithms for *de novo* genome assembly from short reads⁵, we remain remarkably distant from routinely assembling genomes to the standards set by the HGP. For example, the human genome was assembled with less than 40 gigabases (Gb) of Sanger sequencing, but *de novo* assemblies of short reads relying on 5- to 10-fold more sequence are highly fragmented relative to the finished chromosomes of the *H. sapiens* reference build^{6,7}.

It is important to recognize that the high quality of the HGP's genome assemblies is not solely attributable to the length and accuracy of Sanger sequencing reads. Rather, a diversity of approaches was brought to bear to achieve long-range contiguity. For the human genome, this included dense genetic maps, dense physical maps and hierarchical shotgun sequencing of a tiling path of long insert clones^{1,2}. Whole-genome shotgun assemblies – typically based on end sequencing of both short and long insert clones – also relied on dense genetic and physical maps to assign, order and orient sequence contigs or scaffolds to chromosomes⁸.

Diverse strategies have been developed to boost the contiguity of *de novo* genome assemblies from short reads. These include end sequencing of fosmid clones⁶, fosmid clone dilution pool sequencing^{9,10}, optical mapping^{11–14} and genetic mapping with restriction site associated DNA (RAD) tags¹⁵. However, each of these strategies has important limitations. Fosmid libraries and optical mapping are technically challenging and provide only mid-range contiguity. Genetic maps are more powerful but are costly or impractical to generate for many species. Particularly as initiatives such as the 10K Genome Project¹⁶ gain momentum, the genomics field is in need of scalable, broadly accessible methods enabling chromosome-scale *de novo* genome assembly.

Hi-C and related protocols use proximity ligation and massively parallel sequencing to probe the three-dimensional architecture of chromosomes within the nucleus, with interacting regions captured to paired-end reads^{17,18}. In the resulting datasets, the probability of intrachromosomal contacts is on average much higher than that of interchromosomal contacts, as expected if chromosomes occupy distinct territories. Moreover, although the probability of interaction decays rapidly with linear distance, even loci separated by >200 Mb on the same chromosome are more likely to interact than loci on different chromosomes¹⁷.

We speculated that genome-wide chromatin interaction datasets, such as those generated by Hi-C, might provide long-range information about the grouping and linear organization of sequences along entire chromosomes. In exploring this, we developed *LACHESIS* (ligating adjacent chromatin enables scaffolding in situ), a computational method that exploits the signal of genomic proximity in Hi-C datasets for ultra-long-range scaffolding of *de novo* genome assemblies. *LACHESIS* works in three steps (Fig. 1) – first, clustering contigs or scaffolds to chromosome groups; second, ordering contigs or scaffolds within each chromosome group; and finally, assigning relative orientations to individual contigs or scaffolds. We demonstrate the effectiveness of this approach by combining shotgun fragment and short insert mate-pair (<3 Kb) sequences with Hi-C data to generate

reasonably accurate chromosome-scale *de novo* assemblies of the *H. sapiens*, *M. musculus* and *D. melanogaster* genomes. We also show that Hi-C data can be used to validate chromosomal rearrangements in cancer genomes.

Results

The input to *LACHESIS* consists of a set of contigs or scaffolds (the term ‘contig’ is used in this description of the method to indicate both possibilities), such as are generated by de Bruijn graph-based *de novo* assemblers^{5,6}, and a genome-wide chromatin interaction dataset, such as is generated by the Hi-C method^{17,18}. The Hi-C reads are aligned to the contigs, and the number of Hi-C read pairs linking each pair of contigs is tabulated (Figure 1a). In a first step, *LACHESIS* uses hierarchical agglomerative clustering to group contigs that are likely to derive from the same chromosome, exploiting the fact that intrachromosomal contacts are on average more probable than interchromosomal contacts in Hi-C datasets¹⁷ (Fig. 1b; Supplementary Fig. 1). An average-linkage metric¹⁹ is used for this clustering, with linkage defined as the normalized density of Hi-C read-pairs linking any given pair of contigs. The final number of groups is pre-specified, ideally set to the expected number of chromosomes.

In a second step, *LACHESIS* orders contigs linearly within each chromosome group by taking advantage of the higher Hi-C link densities expected between closely located contigs (Fig. 1c; Supplementary Fig. 2). For each chromosome group, a graph is built with vertices representing contigs and edge weights corresponding to the inverse of the normalized Hi-C linkage density between pairs of contigs. A minimum spanning tree (MST) is found in this graph, and the longest path in the MST is extracted as the ‘trunk’, an incomplete but high-confidence ordering of contigs within each chromosome group. To generate a full ordering, contigs excluded from the trunk are reinserted into it at sites that maximize the amount of linkage between adjacent contigs.

In a third step, the ordered contigs are oriented with respect to one another by taking into account precisely where the Hi-C reads map on each contig (Fig. 1d; Supplementary Fig. 3). For each chromosome group, a weighted directed acyclic graph (WDAG) is built representing all possible ways to orient the contigs, given the predicted order. The weights are calculated as the log-likelihood of the observed Hi-C links between adjacent contigs in a given combined orientation, assuming that the probability of a link connecting two reads at a genomic distance of x decays as $1/x$ for $x \sim 100$ Kb¹⁷. The maximum likelihood path through this graph yields a predicted orientation for each contig.

Chromosome-scale assembly of mammalian genomes

We sought to evaluate the effectiveness of this approach for the chromosome-scale *de novo* assembly of mammalian genomes. We focused on human and mouse as test cases because of the availability of the necessary datasets and the high quality of these reference genomes as gold standards for comparison. For human, we used *ALLPATHS-LG* to assemble previously generated⁶ shotgun fragment and short jump (~2.5 Kb) mate-pair sequences to an N50 scaffold length of 437 Kb and a total length of 2.74 Gb. We refer to this below as the

‘shotgun assembly.’ We intentionally excluded fosmid end sequencing data⁶ because libraries of this type require cloning and are laborious to generate. Furthermore, we hoped that the chromatin interaction data would effectively substitute for the ~40 Kb fosmid links while also providing even longer-range contiguity.

After aligning Hi-C read-pairs from a human male ESC line²⁰ to this shotgun assembly, we applied *LACHESIS* to cluster the scaffolds into 23 chromosome groups (the libraries used to generate the shotgun assembly were derived from female DNA⁶), and then to order and orient the scaffolds within each chromosome group (Fig. 2, 3; Table 1; Supplementary Fig. 4; Supplementary Tables 1, 2). Most scaffolds ($n = 13,528$, comprising 98.2% of the length of the shotgun assembly) were clustered into one of the 23 groups (Fig. 2a). Nearly all of these groups corresponded to individual chromosomes, with the exceptions of the X chromosome, whose two arms were split in separate groups (Fig. 3u,v); one chimeric group containing very little sequence from many chromosomes (6.5 Mb total; Supplementary Fig. 4w); chromosomes 19 and 22, which were “fused” into a single group (Fig. 3s); and chromosomes 20 and 21, also fused into a single group (Fig. 3t). The fusions are probably due to the greater density of interchromosomal links observed between short chromosomes in Hi-C data^{17,21}. Apart from these errors, 98.6% of clustered scaffolds (comprising 99.86% of their sum length) were correctly grouped (Table 1), suggesting that Hi-C data are highly informative for the clustering of sequences derived from individual chromosomes, including across centromeres.

Within each chromosome group, the vast majority of the length of the clustered scaffolds was successfully ordered and oriented by *LACHESIS* (94.4% or 2.55 Gb; Table 1). The predicted orderings are highly concordant with the reference human genome (GRCh37), including across most megabase-scale centromere gaps, except for the occasional rearrangement of large segments within which nearly all scaffolds were well-ordered (Fig. 3; Supplementary Fig. 4). For example, scaffolds corresponding to the long and short arms of chromosome 1 are grouped together and respectively very well-ordered, but the reconstructed arms are joined incorrectly (Fig. 2b). To quantify local errors, we defined ordering errors as instances where a contig or scaffold is not in the expected order with respect to its immediate neighbors, and orientation errors as instances where a contig or scaffold is not in the expected orientation implied by its immediate predecessor in the ordering. By these definitions, 99.2% of clustered scaffolds, representing 99.5% of the sum length, were correctly ordered; 97.5% of clustered scaffolds, representing 98.8% of the sum length, were correctly oriented.

Most ordering errors involve the inversion of local segments consisting of one or several contiguous scaffolds (Supplementary Fig. 4). Compared to correctly ordered scaffolds, incorrectly ordered scaffolds are short and are enriched for segmental duplications and simple repeats (Supplementary Fig. 5; Supplementary Table 3). This suggests that complexities in the primary sequence are the source of many ordering errors, possibly via inaccuracies in the shotgun assembly or by confounding the mapping of Hi-C read-pairs. Other errors appear to be associated with the non-uniform distribution of biological interactions, *e.g.*, chromatin domains at various scales (Supplementary Fig. 6). To address this in part, we calculated a quality score for ordering and orientation, defined as the relative

log-likelihood of the contig's predicted orientation to its opposite orientation in the WDAG. Local accuracy was better for scaffolds with high quality scores (Table 1). For scaffolds with high quality scores occurring within the assembly trunk, which comprise 2.09 Gb or 76.4% of the overall shotgun assembly, 99.9% of sequence is correctly ordered and 99.7% correctly oriented (Supplementary Table 1).

We also attempted the chromosome-scale *de novo* assembly of the mouse genome by an identical approach. We first used *ALLPATHS-LG* to assemble previously generated⁶ shotgun fragment and short jump (~2.2 Kb) mate-pair sequences to an N50 scaffold length of 224 Kb and a total length of 2.37 Gb. After aligning Hi-C read-pairs from a mouse ESC line²⁰ to this shotgun assembly, we applied *LACHESIS* to cluster the scaffolds into 20 chromosome groups, and then to order and orient the scaffolds within each chromosome group (Fig. 2c,d; Table 1; Supplementary Fig. 7; Supplementary Tables 1, 4). Most scaffolds ($n = 22,802$, comprising 98.0% of the length of the shotgun assembly) were clustered into one of the 20 groups (Fig. 2c). There was a clear 1-to-1 correspondence between these groups and bona fide chromosomes (GRCm38), although a small part of mouse chromosome 10 (2.6 Mb) was erroneously clustered with chromosome 8 (Supplementary Table 4). Of the clustered scaffolds, 99.5% (comprising 99.76% of their sum length) were correctly grouped (Table 1). The majority of the length of the clustered scaffolds was ordered and oriented by *LACHESIS* (86.7% or 2.02 Gb; Table 1). Almost all (99.5%) of clustered scaffolds, representing 98.9% of the sum length, were correctly ordered; 95.4% of scaffolds, representing 98.1% of the sum length, were correctly oriented. Overall, the results for chromosome-scale *de novo* assembly of the mouse and human genomes are highly consistent.

Chromosome-scale assembly of the fruit fly genome

To further evaluate the generality of this method, we next applied it to the *de novo* assembly of *Drosophila melanogaster*, for which a high-quality reference genome is also available as a gold standard for comparison. We first used *ALLPATHS-LG* to assemble shotgun fragment sequences (without jumping libraries) to an N50 contig length of 68 Kb and a total length of 127 Mb^{6,22}. We then aligned Hi-C read-pairs derived from *D. melanogaster*²³ to this shotgun assembly and used *LACHESIS* to cluster the contigs into 4 chromosome groups. Most contigs (81.2% of the length of the shotgun assembly) were clustered into one of the 4 groups (Supplementary Fig. 8). This proportion is lower than that for the assemblies described above (98% for human and mouse), most likely because of the lower contiguity of the shotgun assembly (N50 contig size of 68 Kb for *Drosophila* versus N50 scaffold size of 437 Kb and 224 Kb for human and mouse, respectively). Nonetheless, the four groups corresponded well to the four *Drosophila* chromosomes (X, 2, 3 and 4), even though chromosome 4 is minuscule compared to the others (1.4 Mb or ~1% of the reference genome). Of the clustered scaffolds, 89.5% (comprising 96.6% of their sum length) were correctly grouped.

We next applied *LACHESIS* to order and orient the *Drosophila* contigs within each of the 4 chromosome groups (Supplementary Table 5; Supplementary Fig. 9). A lower proportion of the shotgun assembly was ordered (82.0% by length for fly versus 94.4% for human), again likely because the *Drosophila* assembly has shorter contigs than the mammalian shotgun

assemblies used above. The predicted order corresponded well with the actual order based on contig alignments to the *D. melanogaster* reference genome (FB2013_02, euchromatic sequences only), and the R and L arms of chromosomes 2 and 3 were well-separated (Supplementary Fig. 9). Once again, a subset of the chromosome groups contained rearrangements of large segments within which nearly all contigs were well-ordered. At a local scale, 94.8% of clustered contigs (95.4% of sum length) were correctly ordered, and 93.9% of clustered contigs (95.9% of sum length) were correctly oriented (Table 1).

Robustness to contig size and Hi-C data quantity

Our results for chromosome-scale scaffolding of the human, mouse and fly genomes were based on initial *de novo* assemblies with reasonably high N50s, *i.e.*, 437 Kb, 224 Kb and 68 Kb, respectively. To evaluate the power of this approach as a function of the contiguity of this initial assembly, we sought to reassemble simulated contigs of varying size derived from the human reference genome (GRCh37). In each iteration, we split the human reference genome into equally sized contigs (10, 20, 50, 100, 200, 500 or 1,000 Kb) and mapped Hi-C read-pairs²⁰ to these simulated shotgun assemblies. We then used *LACHESIS* to cluster, order and orient the simulated contigs (results for 100 Kb simulated contigs are shown in Supplementary Fig. 10, 11). As shown in Table 2, the performance of the method with respect to completeness and local accuracy is robust above an initial N50 of 50 Kb, but degrades rapidly below this point.

In a separate analysis, we down-sampled the sequencing depth of Hi-C data and attempted chromosome-scale scaffolding of the human shotgun assembly (N50 = 437 Kb; Supplementary Table 6). Although clustering is robust to marked reductions in the amount of Hi-C data, accurate ordering and orienting of scaffolds within chromosome groups requires ~400M read-pairs. Nonetheless, we note that even the full amount of Hi-C data used here is less than 20% of the amount of sequencing data used to generate the initial shotgun assembly (59 Gb vs. 303 Gb).

Validating translocations in cancer genomes

We also speculated that the strong intrachromosomal signal observed in Hi-C data might enable the global discovery or validation of interchromosomal rearrangements in cancer genomes, many of which are challenging to detect with methods other than karyotyping because the breakpoints occur in repetitive regions. For example, recent studies combined several mate-pair sequencing strategies to detect rearranged marker chromosomes in the aneuploid HeLa cancer cell line^{24,25}, but such methods were only successful for a small proportion of rearrangements, and for none of the rearrangements involving centromeric sequences. Of note, the 4C method was previously used to detect chromosomal breakpoints in cancer genomes, but in a targeted rather than global fashion²⁶.

To test this, we constructed a Hi-C library from HeLa cells and sequenced it to high depth (154 M unique read-pairs). These data were used to generate a matrix of link densities between ~1 Mb windows in the human reference genome. Visual examination of the matrix revealed off-diagonal patches of strong linkage with asymmetric decay, consistent with interchromosomal rearrangements (Fig. 4). Most of these corresponded well to previously

described marker chromosomes²⁷, although we also observed strong evidence for two novel marker chromosomes (der(2;7)(q36;q10), “U1” and der(3;20)(q25;q10), “U2”). We implemented a rearrangement-calling method that successfully identified all of the suspected marker chromosomes, albeit with limited specificity (Supplementary Fig. 12). Using chromatin interaction data in this way may enable the validation of candidate chromosomal rearrangements, or the detection of chromosomal rearrangements in heterogeneous cancer cell populations that might not be detected by karyotyping of limited numbers of cells.

Discussion

Here we demonstrate that genome-wide chromatin interaction datasets, such as those generated by Hi-C, are a rich source of long-range information for assigning, ordering and orienting genomic sequences to chromosomes, including across megabase-scale centromere gaps, as well as for validating chromosomal translocations in cancer genomes. There are a number of avenues for the potential improvement of this approach, both experimentally and computationally.

Although the experimental methods for Hi-C are straightforward, current protocols require a large amount of material (10^6 – 10^8 cells). As such, reducing the input requirements is an important technical goal. To date, global chromatin interaction datasets have been generated on organisms including yeast¹⁸, human^{17,20,21}, mouse²⁰, fruit fly²³ and *Arabidopsis thaliana*²⁸. This is consistent with broad applicability, but demonstrating these protocols on an even more diverse range of organisms is imperative. On a related point, as the success of this approach depends on chromosomes occupying distinct territories in the nucleus, it will be important to further validate *LACHESIS* in diverse species to confirm that this is ubiquitously the case. We also note that using multiple restriction enzymes (or developing new methods that avoid restriction digestion altogether) will likely improve performance, particularly for smaller contigs or scaffolds. Along the same lines, even if this approach broadly enables chromosome-scale scaffolding, the contiguity required for the initial *de novo* assembly (~50 Kb) may be challenging to achieve for many organisms. As such, there will remain a strong need for methods delivering “intermediate” contiguity information in a highly cost-effective and scalable manner.

Computationally, a substantial limitation of our current algorithm is that the clustering step requires the number of chromosomal groups to be specified *a priori*. We assessed whether the scoring metric used during clustering enables reliable inference of chromosome number, but this is not the case (Supplementary Fig. 13). One potential solution is to order contigs or scaffolds prior to determining chromosome groups, but this is computationally difficult with large numbers of contigs or scaffolds. Alternatively, statistical methods for predicting the optimal number of clusters may prove useful^{29,30}.

Ordering and orientation errors were associated with short scaffolds, segmental duplications and simple repeats (Supplementary Table 3). It is possible that our full exclusion of ambiguously mapping reads may be introducing ‘gaps’ in contiguity information that increase the probability of errors in such regions. Alternatively, these errors may be secondary to flaws in the initial shotgun assembly. Consistent with the latter, we also ran

LACHESIS on a human ‘shotgun assembly’ that has higher contiguity because it used fosmid end-pair data⁶ (N50 scaffold length 11.5 Mb versus 437 Kb). We achieved chromosome-scale scaffolding of this assembly as well, but with lower accuracy owing to a small fraction of incorrectly joined scaffolds in the input to *LACHESIS* (Supplementary Table 1). This suggests that conservative *de novo* assembly prior to using chromatin interaction mapping for long-range scaffolding may be optimal. Lastly, we note that our use of chromatin interaction data for long-range scaffolding (via *LACHESIS*) was entirely separate from the initial assembly of contigs/scaffolds (by *ALLPATHS-LG*). We anticipate that a more integrated approach might improve accuracy.

Starting from draft human and mouse genome assemblies, each consisting of tens of thousands of scaffolds, we were able to cluster nearly all scaffolds into groups that overwhelmingly corresponded to individual chromosomes. A high fraction of these assignments were correct (comprising >99% of the sum length of clustered scaffolds). We were further able to order and orient contigs within each chromosome group, including scaffolding across megabase-scale centromere gaps, with surprisingly few errors. As such, we achieved reasonably accurate *de novo* mammalian genome assemblies with chromosome-scale contiguity using just three types of libraries, all generated by *in vitro* methods and sequenced as short read-pairs on a single platform (for human, shotgun fragment (161 Gb); ~2.5 Kb short jump (142 Gb); and Hi-C (59 Gb)). Although its broad applicability beyond the genomes assembled here has still to be demonstrated, our approach may enable a new generation of *de novo* genome assemblies that do not sacrifice the high standards for contiguity set by the HGP.

Online Methods

Input datasets

In the Hi-C procedure¹⁷, DNA in a nucleus is crosslinked, then cut with a restriction enzyme, leaving pairs of distally located but physically associated DNA molecules attached to one another. The sticky ends of these fragments are biotinylated and then ligated to each other to form chimeric circles. Biotinylated circles are enriched for, sheared again, and then processed to sequencing libraries in which individual templates are chimeras of the physically associated DNA molecules from the original cross-linking.

Four Hi-C datasets were used, corresponding to human cells, mouse cells, *Drosophila melanogaster* tissue and HeLa cells. The human dataset was produced from human embryonic stem cells (hESCs)²⁰. The hESC replicates 1 and 2 were used (NCBI SRA accessions: GSM862723, GSM892306) for a total of 734 M read-pairs. The mouse dataset was produced from mouse embryonic stem cells (mESCs)²⁰. The mESC replicates 1 and 2 were used (NCBI SRA accessions: GSM862720, GSM862721) for a total of 806 M read-pairs. The *D. melanogaster* dataset was produced from embryos²³ and includes 363 M read-pairs (NCBI SRA accession: SRX111555). The HeLa dataset was produced as part of this study (see “Chromosome Fusion Detection in HeLa”, below) and includes 305 M read-pairs.

Two types of shotgun assemblies were created as inputs to *LACHESIS*. First, we created shotgun assemblies for human, mouse and *Drosophila melanogaster* by downloading the

appropriate sequence libraries from SRA and assembling them with *ALLPATHS-LG*. Table 1 shows statistics for these three assemblies. Second, simulated shotgun assemblies were made by breaking up the human reference genome into contigs of varying sizes, ranging from 10 Kb to 1 Mb. Table 2 shows statistics for these assemblies.

Shotgun assemblies

To create the human shotgun assembly, we downloaded the sequence files⁶ corresponding to the fragment library and two short jumping libraries for individual NA12878 from the NCBI Short Read Archive (NCBI SRA accession SRA024407). The files were converted from sra to fastq format, and formatted as required by the *ALLPATHS-LG* assembler using the PrepareAllPathsInputs.pl script included with the *ALLPATHS-LG* distribution. The reads were assembled using the *ALLPATHS-LG* assembler⁶ (version r41985) with the following parameters (the rest being default): HAPLOIDIFY = TRUE, MAX_MEMORY_GB = 400, THREADS = 32, EVALUATION = STANDARD. Insert size estimates (mean and standard deviation) for each library were specified based on the values provided previously⁶. Scaffolds in this assembly were treated as contigs by *LACHESIS*. Because we intentionally excluded fosmid end sequencing data, this assembly had far less mid-range contiguity than the full *de novo* assembly produced previously⁶ (N50 scaffold length 437 Kb versus 11.5 Mb), and thus it more closely represents a typical *de novo* assembly created exclusively from *in vitro* libraries.

To create the mouse shotgun assembly, we downloaded the sequence files⁶ corresponding to the fragment and three short jumping libraries from the NCBI Short Read Archive (NCBI SRA accession SRA009956). The libraries were assembled using the *ALLPATHS-LG* assembler⁶ (version r41985) with the following parameters (the rest being default): HAPLOIDIFY = TRUE, MAX_MEMORY_GB = 500, THREADS = 32. Insert size estimates (mean and standard deviation) for each library were specified based on the values provided previously⁶.

To create the *Drosophila melanogaster* shotgun assembly, we downloaded the sequence files for *D. melanogaster* (Drosophila Genomic Reference Panel²² corresponding to sequencing runs SRR516038 (Sample DGRP-348) and SRR516001 (Sample DGRP-821) from the NCBI Short Read Archive. SRR516038 served as the “fragment” library as per *ALLPATHS-LG* terminology. The *ALLPATHS-LG* assembler also requires a “jumping” library. We were unable to find a previously sequenced jumping library for *D. melanogaster*. As a work-around, we used a standard shotgun library with a slightly higher insert size (SRR516001) and artificially converted it into a jumping library by flipping the orientation of reads. All files were first converted from sra to fastq format, then formatted as required by the *ALLPATHS-LG* assembler using the PrepareAllPathsInputs.pl script included with the *ALLPATHS-LG* distribution. Insert size distributions for these libraries (mean = 205bp, standard deviation = 25bp for fragment library; mean = 320bp, standard deviation = 52bp for jumping library) were obtained by aligning a subset of reads to the *D. melanogaster* reference genome using BWA³¹. The reads were assembled using the *ALLPATHS-LG* assembler⁶ (version r41985) with the following parameters (the rest being

default): HAPLOIDIFY = TRUE, MAX_MEMORY_GB = 300, THREADS = 16, VAPI_WARN_ONLY=True.

Aligning Hi-C reads

Hi-C reads were aligned to shotgun assemblies or reference genomes using BWA³¹ with default parameters. Reads were considered artifactual if they did not align within 500 bp of a restriction site, as recommended²¹. Non-uniquely aligning reads were assigned a mapping quality of 0 by BWA and were excluded from subsequent analysis. Additionally, read-pairs were considered for downstream analysis only if both reads in the pair aligned to contigs from the assembly.

Clustering contigs or scaffolds into chromosome groups

Contigs or scaffolds (the term ‘contig’ is used in this description of the method to indicate both possibilities) were placed into groups using hierarchical clustering (Supplementary Fig. 1). A graph was built, with each node initially representing one contig, and each edge between nodes having a weight equal to the number of Hi-C read-pairs linking the two contigs. The contigs were merged together using hierarchical agglomerative clustering with an average-linkage metric¹⁹, which was applied until the number of groups was reduced to the expected number of distinct chromosomes (counting only groups with more than one contig). Repetitive contigs (contigs whose average link density with other contigs, normalized by number of restriction fragment sites, was greater than two times the average link density) and contigs with too few restriction fragment sites (<5 for the simulated human assembly; <25 for the human and mouse *de novo* assemblies; <250 for the *D. melanogaster* assembly) were not clustered. However, after clustering, each of these contigs was assigned to a group if its average link density with that group was greater than four times its average link densities with any other group.

Ordering contigs or scaffolds within chromosome groups

Each group of contigs or scaffolds (the term ‘contig’ is used in this description of the method to indicate both possibilities) was ordered using the following algorithm (Supplementary Fig. 2). First, a graph was built as in the clustering step, but with the edge weights between nodes equal to the inverse of the number of Hi-C links between the contigs, normalized by the number of restriction fragment sites per contig. Short contigs (<5 restriction fragment sites for the simulated human assemblies; <20 sites for the human and mouse *de novo* assemblies; <20 Kb for the *Drosophila de novo* assembly) were excluded from this graph. A minimum spanning tree was calculated for this graph. The longest path in this tree, the “trunk”, was found. The spanning tree was then modified so as to lengthen the trunk by adding to it contigs adjacent to the trunk, in ways that kept the total edge weight heuristically low.

After a lengthened trunk was found for each group, it was converted into a full ordering as follows. The trunk was removed from the spanning tree, leaving a set of “branches” containing all contigs not in the trunk. These branches were reinserted into the trunk, the longest branches first, with the insertion sites chosen so as to maximize the number of links between adjacent contigs in the ordering. Short fragments (<5 restriction fragment sites for

the simulated human assemblies; <20 sites for the human and mouse *de novo* assemblies; <40 Kb for the *Drosophila de novo* assembly) were not reinserted; as a result, many small contigs that were clustered were left out of the final *LACHESIS* assembly.

Orienting contigs or scaffolds

The orientation of each contig or scaffold (the term ‘contig’ is used in this description of the method to indicate both possibilities) within its ordering was determined by taking into account the exact position of the Hi-C link alignments on each contig (Supplementary Fig. 3). It was assumed that, as demonstrated in previous Hi-C studies¹⁷, the likelihood of a Hi-C link connecting two reads at a genomic distance of x is roughly $1/x$ for $x \sim 100$ Kb. A weighted directed acyclic graph (WDAG) was built representing all possible ways to orient the contigs in the given order. Each edge in the WDAG corresponded to a pair of adjacent contigs in one of their four possible combined orientations, and the edge weight was set to the log-likelihood of observing the set of Hi-C link distances between the two contigs, assuming they were immediately adjacent with the given orientation.

For each contig, a quality score for its orientation was calculated as follows. The log-likelihood of the observed set of Hi-C links between this contig, in its current orientation, and its neighbors, was found. Then the contig was flipped and the log-likelihood was calculated again. The first log-likelihood was guaranteed to be higher because of how the orientations were calculated. The difference between the log-likelihoods was taken as a quality score.

Validation

To determine the true position of the contigs or scaffolds in the shotgun assemblies, we aligned them to the human, mouse or *D. melanogaster* reference genome using BLASTn³² with parameters ‘-perc_identity 99 -evalue 100 -word_size50’. For each contig, a “truth placement” on reference was derived as follows. First, the chromosome was chosen containing the plurality of aligned sequence from the contig. Second, the single best alignment to this chromosome (measured by E-value) was used to “seed” a chromosomal region. Third, the other alignments to this chromosome were considered by descending E-value, and the region was extended to include as many of them as possible without exceeding the total length of the assembly contig.

Chromosome Fusion Detection in HeLa

A single, complex Hi-C library was constructed for the HeLa S3 cancer cell line (ATCC CCL2.2; grown in DMEM with 10% FBS and 1X Pen. Strep.) according to a published³³ protocol. This library was sequenced on two lanes of Illumina HiSeq 2000, followed by read trimming to 50 bp to eliminate ligation-spanning reads that confound alignment. Reads were aligned to the human reference genome using BWA³¹ with default parameters, followed by removal of PCR duplicates. Reads were then assigned to genomic windows containing approximately one megabase of sequence (mean = 955,176 bp) that were determined by bases of unique mappability to the genome. Links between windows were normalized first to the number of HindIII restriction sites present in the window to account for biases inherent to restriction based library preparation, then to the total count of short pairs within

the window (defined as pairs with an insert size ± 1 Kb) to account for the underlying copy number of the window.

Rearrangements were called by first identifying stretches of ± 10 consecutive windows within a row where $\geq 80\%$ of windows have a link score ≥ 1 standard deviation above the mean of the entire row. Stretches of windows present in columns were called using the same parameters. Windows present in outlier stretches for both rows and columns were defined as outlier windows. These windows were then clustered with all proximal windows ± 2 windows away and the outlier window count and density within the outer borders of the cluster determined. Outlier spans and clusters are shown in Supplementary Fig. 12.

Software Availability

The *LACHESIS* software was written in C++ using Boost (<http://www.boost.org/>) and includes auxiliary scripts written in Perl. It runs in a Unix environment. A distribution of the *LACHESIS* source code is included as Supplementary Data File 1 (*LACHESIS.tar.gz*) and a documentation and user's guide are included as Supplementary Data File 2 (*README.txt*). Both of these files are also freely available for public download at <http://www.gs.washington.edu/~jnburton/LACHESIS/Updated> versions of the source code will also be made available there.

Supplementary Material

Refer to Web version on PubMed Central for supplementary material.

Acknowledgments

We thank F. Ay, J. Felsenstein, P. Green, W. Noble, R. Waterston and members of the Shendure Lab for helpful discussions. Some of the sequencing data used in this research was derived from a HeLa cell line. Henrietta Lacks, and the HeLa cell line that was established from her tumor cells without her knowledge or consent in 1951, have made significant contributions to scientific progress and advances in human health. We are grateful to Henrietta Lacks, now deceased, and to her surviving family members for their contributions to biomedical research. The HeLa associated genomic datasets described in this manuscript are available via the database of Genotypes and Phenotypes (dbGaP) as a substudy of the HeLa Cell Genome Sequencing Studies, phs000640. Our work was supported by grant HG006283 from the National Human Genome Research Institute (NHGRI; to J.S.); a graduate research fellowship DGE-0718124 from the National Science Foundation (to A.A. and J.O.K.); and grant T32HG000035 from the NHGRI (to J.N.B.).

References

1. International Human Genome Sequencing Consortium. Initial sequencing and analysis of the human genome. *Nature*. 2001; 409:1–62. [PubMed: 11343073]
2. International Human Genome Sequencing Consortium. Finishing the euchromatic sequence of the human genome. *Nature*. 2004; 431:931–945. [PubMed: 15496913]
3. Shendure J, Ji H. Next-generation DNA sequencing. *Nature Biotechnology*. 2008; 26:1–11.
4. Shendure J, Lieberman-Aiden E. The expanding scope of DNA sequencing. *Nature Biotechnology*. 2012; 30:1084–94.
5. Compeau P, Pevzner P, Tesler G. How to apply de Bruijn graphs to genome assembly. *Nature Biotechnology*. 2011; 29:987–91.
6. Gnerre S, et al. High-quality draft assemblies of mammalian genomes from massively parallel sequence data. *Proceedings of the National Academy of Sciences of the United States of America*. 2011; 108:1–6.

7. Li R, et al. *De novo* assembly of human genomes with massively parallel short read sequencing. *Genome Research*. 2010; 20:265–272. [PubMed: 20019144]
8. Mouse Genome Sequencing Consortium. Initial sequencing and comparative analysis of the mouse genome. *Nature*. 2002; 420:1–43.
9. Kitzman JO, et al. Haplotype-resolved genome sequencing of a Gujarati Indian individual. *Nature Biotechnology*. 2011; 29:1–6.
10. Zhang G, et al. The oyster genome reveals stress adaptation and complexity of shell formation. *Nature*. 2012; 490:49–54. [PubMed: 22992520]
11. Schwartz DC, et al. Ordered restriction maps of *Saccharomyces cerevisiae* chromosomes constructed by optical mapping. *Science*. 1993; 262:110–4. [PubMed: 8211116]
12. Zhang Q, et al. The genome of *Prunus mume*. *Nature Communications*. 2012; 3:1318.
13. Dong Y, et al. Sequencing and automated whole-genome optical mapping of the genome of a domestic goat (*Capra hircus*). *Nature Biotechnology*. 2013; 31:135–41.
14. Lam E, et al. Genome mapping on nanochannel arrays for structural variation analysis and sequence assembly. *Nature Biotechnology*. 2012; 30:771–6.
15. Baird NA, et al. Rapid SNP discovery and genetic mapping using sequenced RAD markers. *PLoS One*. 2008; 3:e3376. [PubMed: 18852878]
16. Genome 10K Community of Scientists. Genome 10K: a proposal to obtain whole-genome sequence for 10,000 vertebrate species. *The Journal of Heredity*. 2009; 100:659–74. [PubMed: 19892720]
17. Lieberman-Aiden E, et al. Comprehensive mapping of long-range interactions reveals folding principles of the human genome. *Science*. 2009; 326:289–293. [PubMed: 19815776]
18. Duan Z, et al. A three-dimensional model of the yeast genome. *Nature*. 2010; 465:363–7. [PubMed: 20436457]
19. Eisen M, Spellman P, Brown P, Botstein D. Cluster analysis and display of genome-wide expression patterns. *Proceedings of the National Academy of Sciences of the United States of America*. 1998; 95:14863–8. [PubMed: 9843981]
20. Dixon J, et al. Topological domains in mammalian genomes identified by analysis of chromatin interactions. *Nature*. 2012; 485:376–80. [PubMed: 22495300]
21. Yaffe E, Tanay A. Probabilistic modeling of Hi-C contact maps eliminates systematic biases to characterize global chromosomal architecture. *Nature Genetics*. 2011; 43:1059–65. [PubMed: 22001755]
22. Mackay T, et al. The *Drosophila melanogaster* Genetic Reference Panel. *Nature*. 2012; 482:173–8. [PubMed: 22318601]
23. Sexton T, et al. Three-dimensional folding and functional organization principles of the *Drosophila* genome. *Cell*. 2012; 148:458–72. [PubMed: 22265598]
24. Landry J, et al. The genomic and transcriptomic landscape of a HeLa cell line. *Genes | Genomes | Genetics*. 2013; 1–27. [PubMed: 23316433]
25. Adey A, et al. The haplotype-resolved genome and epigenome of the aneuploid HeLa cancer cell line. *Nature*. 2013; 500:207–211. [PubMed: 23925245]
26. Simonis M, et al. High-resolution identification of balanced and complex chromosomal rearrangements by 4C technology. *Nature Methods*. 2009; 6:837–42. [PubMed: 19820713]
27. Macville M, et al. Comprehensive and definitive molecular cytogenetic characterization of HeLa cells by spectral karyotyping. *Cancer Research*. 1999; 59:1–11.
28. Moissiard G, et al. MORC family ATPases required for heterochromatin condensation and gene silencing. *Science*. 2012; 336:1448–51. [PubMed: 22555433]
29. Fraley C, Raftery AE. How Many Clusters? Which Clustering Method? Answers Via Model-Based Cluster Analysis. *The Computer Journal*. 1998; 41:578–588.
30. Jung Y, Park H, Du DZ, Drake B. A decision criterion for the optimal number of clusters in hierarchical clustering. *Journal of Global Optimization*. 2003; 1–21.
31. Li H, Durbin R. Fast and accurate long-read alignment with Burrows-Wheeler transform. *Bioinformatics*. 2010; 26:589–95. [PubMed: 20080505]

32. Altschul SF, Gish W, Miller W, Myers EW, Lipman DJ. Basic local alignment search tool. *Journal of Molecular Biology*. 1990; 215:403–10. [PubMed: 2231712]
33. van Berkum NL, et al. Hi-C: a method to study the three-dimensional architecture of genomes. *Journal of Visualized Experiments*. 2010:1–7. [PubMed: 20164822]

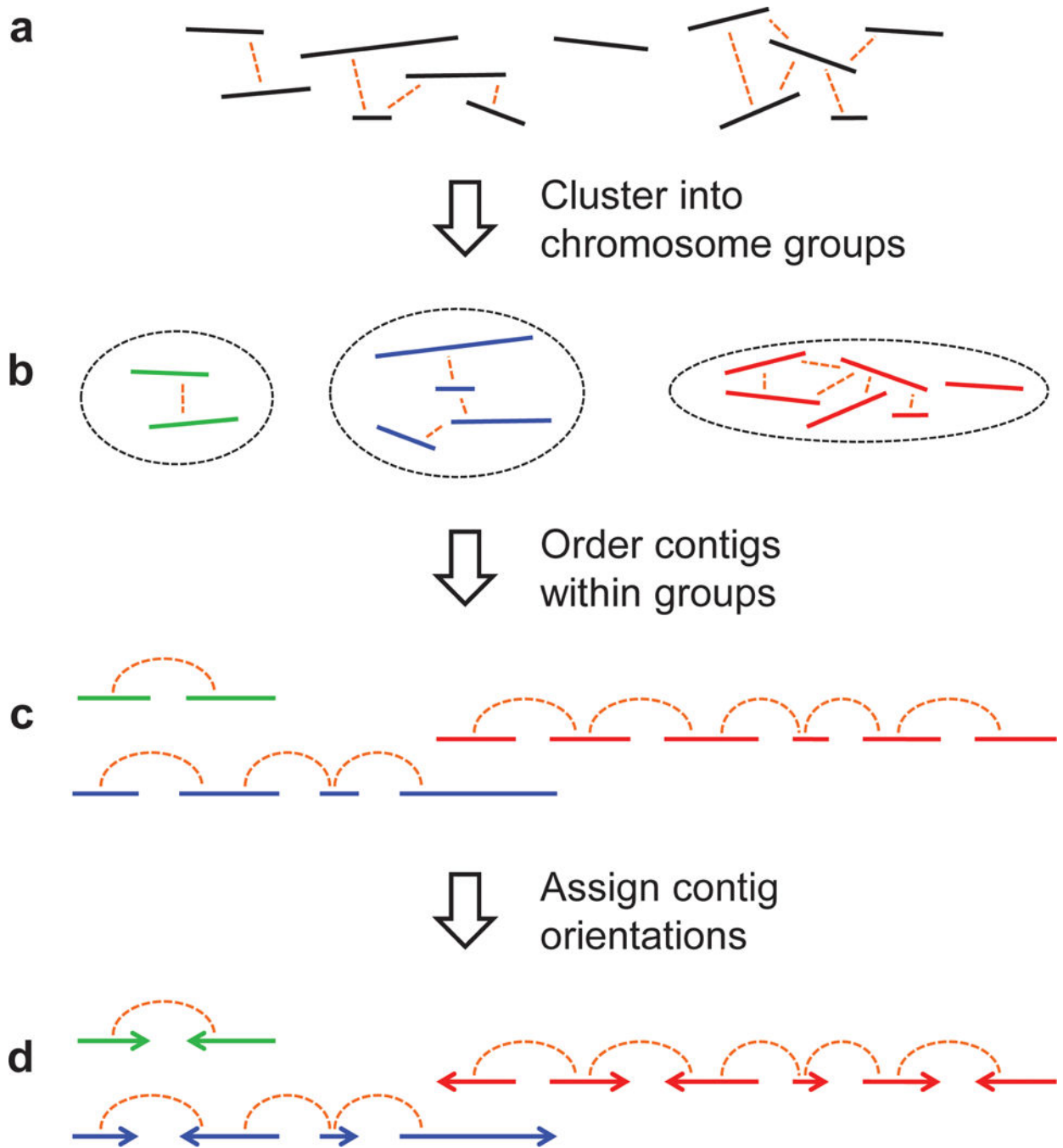


Figure 1.

A schematic of the *LACHESIS* scaffolding method. **(a)** The input consists of a set of contigs (or scaffolds) from a draft assembly and a set of genome-wide chromosome interaction data, *e.g.*, Hi-C links. **(b)** Contigs on the same chromosome tend to have more Hi-C links between them, relative to contigs on different chromosomes. *LACHESIS* exploits this to cluster the contigs into groups that largely correspond to individual chromosomes. **(c)** Within a chromosome, contigs in close proximity tend to have more links than contigs that are distant. *LACHESIS* exploits this to order the contigs within each chromosome group. **(d)**

Lastly, *LACHESIS* uses the exact position of links between adjacent contigs to predict the relative orientation of each contig.

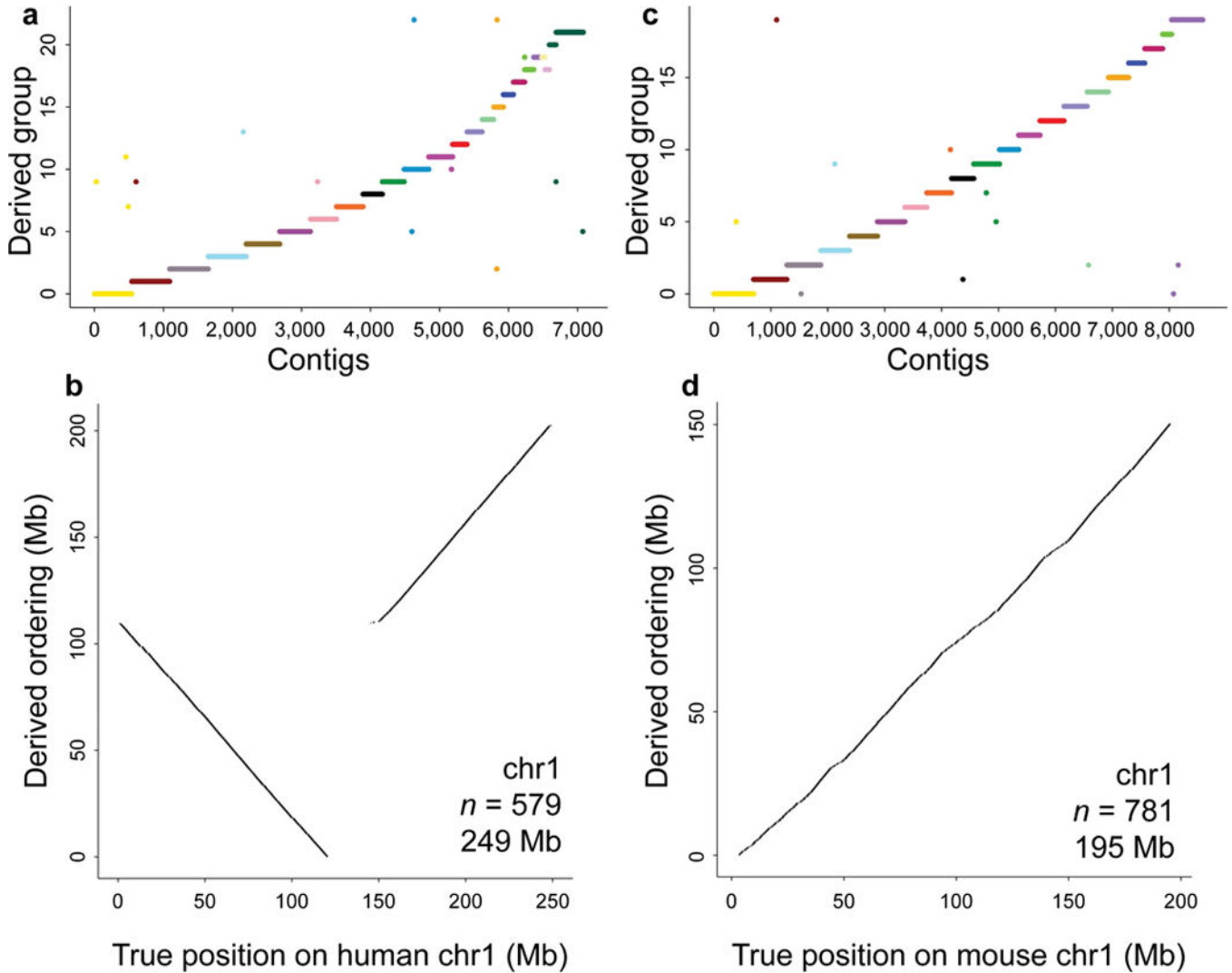


Figure 2.

Clustering and ordering mammalian sequences with *LACHESIS*. (a) The results of *LACHESIS* clustering on the *de novo* human assembly. Shown on the x-axis are the 7,083 scaffolds (total length: 2.49 Gb) that are large (> 25 AAGCTT restriction sites) and not repetitive (Hi-C link density less than 2 times average), which *LACHESIS* uses as informative for clustering. The y-axis shows the 23 groups created by *LACHESIS*, with the order chosen for the purposes of clarity. The color scheme is the standard SKY (spectral karyotyping) color scheme for human. (b) The results of *LACHESIS* ordering and orienting of 579 scaffolds within the group from (a) corresponding to human chromosome 1. On the x-axis is the true position of these scaffolds along human chromosome 1. On the y-axis is the order in which *LACHESIS* has placed these scaffolds. Also listed in the panel are the chromosome name, the number of scaffolds in the derived ordering and the reference length of this chromosome. (c) The results of *LACHESIS* clustering on the *de novo* mouse assembly. Shown on the x-axis are the 8,594 scaffolds (total length: 1.94 Gb) that are large and not repetitive, which *LACHESIS* uses as informative for clustering. The y-axis shows the 20 groups created by *LACHESIS*, with the order chosen for the purposes of clarity. The color

scheme is as in **a**. **(d)** The results of *LACHESIS* ordering and orienting of 781 scaffolds within the group from **c** corresponding to mouse chromosome 1. The plotting is as in **b**.

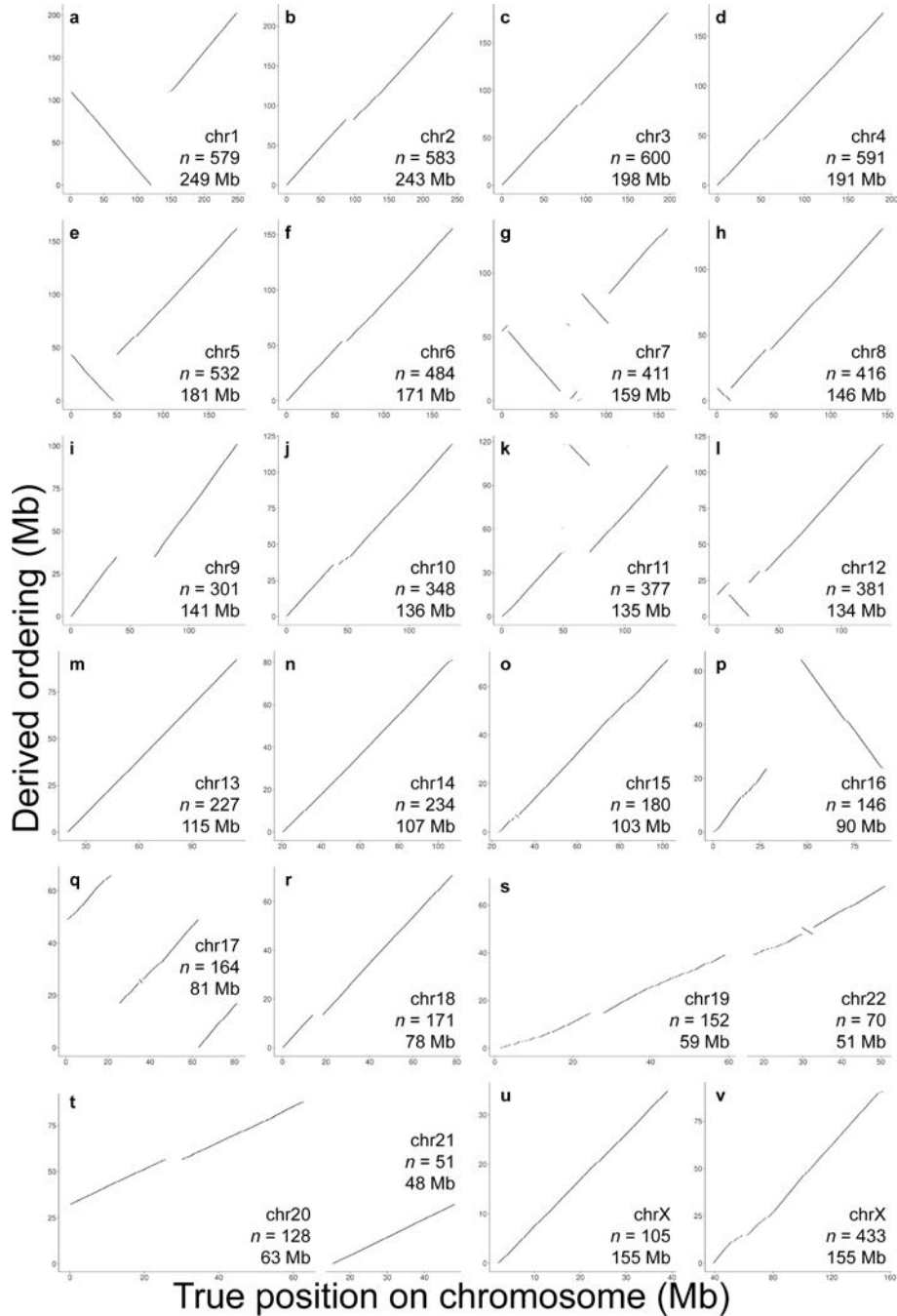


Figure 3. LACHESIS ordering of scaffolds in a *de novo* human assembly. (a–v) The results of LACHESIS ordering and orienting on 22 of the 23 chromosome groups in the *de novo* human assembly. For each ordering, only the scaffolds on the “dominant chromosome” (the chromosome containing the plurality of aligned sequence) are shown. The exceptions are two groups that correspond to fusions of small chromosomes (19 and 22 (s); 20 and 21 (t)) (see Supplementary Table 2). Within each of these fused groups, the two chromosomes were well separated by ordering (s,t). The X chromosome clustered into two separate groups

(**u,v**). Not shown is one very small chimeric group (length = 6.5 Mb; see Supplementary Fig. 4w). Also listed in each panel are the identity of the dominant chromosome, the number of scaffolds in the derived ordering and the reference length of the dominant chromosome.

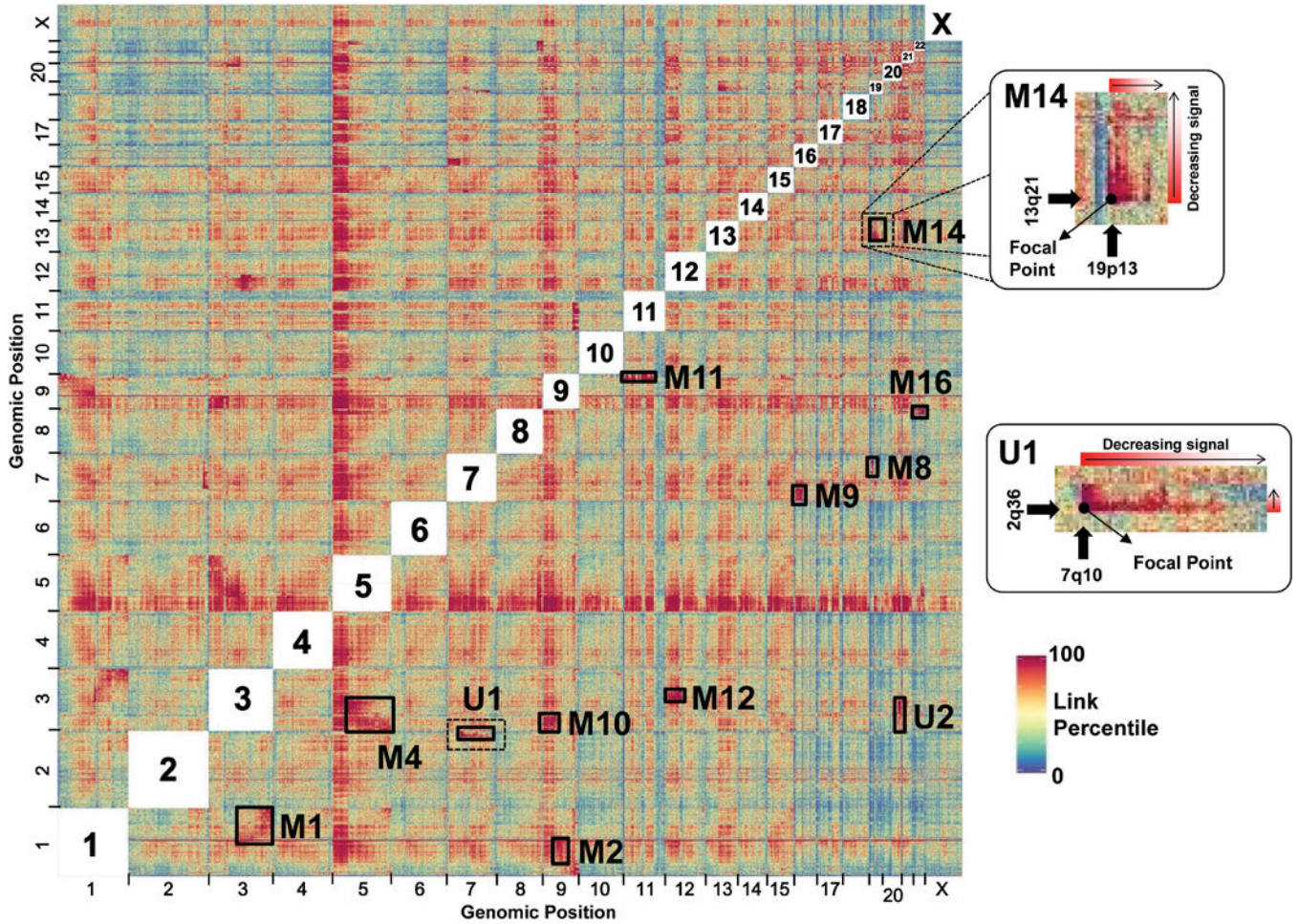


Figure 4. Detection of chromosome fusions in HeLa S3 using Hi-C data. Normalized interchromosomal links for a HeLa S3 Hi-C library between megabase windows were derived as described in Online Methods and are represented as an all-by-all heatmap. For visualization purposes, link weights were ranked and converted to a percentile. Previously identified marker chromosomes were identified (M1, M2, M4, M8, M9, M10, M11, M12, M14 and M16) as well as two additional peaks representing previously undescribed marker chromosomes (U1: der(2;7)(q36;q10) and U2: der(3;20)(q25;q10)). Two rearrangements are highlighted (M14 and U1) to demonstrate the signal focal point at the location of the fusion event with asymmetrical signal decay outward in the direction of the sequence contained in the chromosome fusion, thus allowing breakpoint identification as well as orientation.

Table 1
Metrics for *LACHESIS*-based scaffolding of shotgun assemblies

The human and mouse shotgun assemblies are based on read-pairs from short-insert and ~2.5 Kb jumping libraries, while the *Drosophila* shotgun assembly is based solely on read-pairs from short-insert libraries⁶. The human and mouse shotgun assemblies consist of scaffolds, whereas the *Drosophila* shotgun assembly consists of contigs. *LACHESIS* places scaffolds or contigs into groups and then orders and orients them within each group. An ordering error means that a contig or scaffold's position is out of the expected order with respect to its neighbors. An orientation error means that its orientation is not the orientation implied by its position with respect to its immediate predecessor. 'High-quality predictions' refers to a subset of contigs or scaffolds whose position and orientation in their ordering is deemed more certain; the threshold for high quality is chosen for convenience for each assembly.

Metric	<i>De novo</i> assemblies		
	Human	Mouse	<i>Drosophila</i>
Shotgun assembly metrics			
Total assembly length, including gaps (Mb)	2,739	2,370	127
Number of contigs or scaffolds	18,921	25,964	7,109
N50 contig or ungapped scaffold size (Kb)	437	224	68
Clustering			
% sequence (% contigs) clustered into groups	98.2% (71.5%)	98.0% (87.8%)	81.2% (64.3%)
% clustered sequence (% contigs) mis-clustered	0.14% (1.4%)	0.24% (0.5%)	3.4% (10.5%)
Ordering			
% clustered seq. (% contigs) ordered	94.4% (55.3%)	86.7% (42.7%)	82.0% (24.5%)
% ordered seq. (% contigs) w/ ordering errors	0.5% (0.8%)	0.5% (1.1%)	4.6% (5.2%)
% ordered seq. (% contigs) w/ orientation errors	1.2% (2.5%)	1.9% (4.6%)	4.1% (6.1%)
High-quality predictions			
% ordered seq. (% contigs) w/ high quality	92.8% (79.0%)	93.3% (82.9%)	94.1% (88.1%)
% high-quality seq. (% contigs) w/ ordering errors	0.3% (0.4%)	0.3% (0.7%)	3.3% (3.4%)
% high-quality seq. (% contigs) w/ orientation errors	0.4% (0.5%)	0.5% (1.0%)	2.5% (2.7%)

Table 2
Metrics for *LACHESIS*-based scaffolding of simulated assemblies

Simulated assemblies were created by breaking up the human reference genome into simulated contigs of varying sizes, and then using *LACHESIS* to cluster, order and orient the simulated contigs. The simulated contigs' expected order and orientation are derived from their true position in the reference genome. Ordering and orientation errors are defined as in Table 1.

Metric	Simulated contig size						
	10 Kb	20 Kb	50 Kb	100 Kb	200 Kb	500 Kb	1 Mb
Number of contigs	309,579	154,794	61,927	30,970	15,489	6,206	3,113
% sequence clustered into groups	30.1%	74.2%	91.9%	92.7%	92.9%	93.1%	93.4%
% clustered sequence mis-clustered	1.6%	0.47%	0.41%	0.46%	0.66%	0.66%	0.26%
% clustered sequence ordered	48.5%	79.9%	98.9%	99.8%	99.97%	99.93%	99.98%
% ordered sequence w/ ordering errors	37.2%	18.0%	4.4%	2.2%	1.4%	0.8%	0.8%
% ordered sequence w/ orientation errors	44.8%	28.7%	7.7%	2.6%	1.2%	0.8%	0.7%